Poincaré disk as a model of squeezed states of a harmonic oscillator

Ian Chi
University of California, Davis
Undergraduate Thesis
Spring 2024
Supervisor: Martin Fraas

June 4, 2024

Abstract

Single-mode squeezed states exhibit a direct correspondence with points on the Poincaré disk. In this study, we delve into this correspondence and describe the motions of the disk generated by a quadratic Hamiltonian. This provides a geometric representation of squeezed states and their evolution. We discuss applications in bang-bang and adiabatic control problems involving squeezed states.

Contents

1 Introduction

Geometric representations of quantum states constitute essential tools of quantum mechanics. Widely employed examples include the Bloch sphere representation for qubits [5, 7] and the complex plane representation for coherent states [8], both extensively detailed in quantum mechanics textbooks. The Bloch sphere captures the states of a two-level system in a one-to-one manner. For systems beyond two levels, a comprehensive representation in low-dimensional space becomes impossible. However, it is still possible to represent a sub-manifold, such as the aforementioned coherent states. Another option is to represent classes of states, e.g. states of two qubits modulo local unitary [1]. These geometric representations serve as frameworks, enabling us to conceptualize quantum states and their dynamic evolution through classical analogies. A comprehensive reference for geometric representations is a book [4] and a review [2].

This study delves into the representation of ground states of quadratic Hamiltonians, commonly referred to as squeezed states. We show that squeezed states can be represented on the Poincaré disk model of hyperbolic geometry. Within this mapping, the evolution of squeezed states corresponds to motions of the disk. We demonstrate the utility of the representation by solving some associated control problems.

The representation of squeezed states on the Poincaré was first explored in [3], where it was used to visualize adiabatic crossing of a point where infinitely many eigenvalues collide. In this paper we describe this correspondence in more details. For the sake of completeness we reproduce some results from [3] in the appendix.

2 Background

For clarity, let us cover some of the basic terms that will be used repeatedly in this paper. The first subsection of the background will cover some terms related to the quantum mechanical aspect of the paper, and the second subsection will cover some basic concepts concerning the mathematical aspects concerning Möbius transformations.

2.1 Squeezed Coherent States

Coherent states are a special type of quantum state of the quantum harmonic oscillator in which said state closely mimics the classical behavior of the harmonic oscillator. More formally, they are the states that are the eigenvectors of the creation and annihilation operators.

The annihilation and creation operators are usually denoted as $(\hat{a}^*, \hat{a})$ (in this introduction section the hat refers to operators, but the rest of the paper will suppress these hats for these operators) respectively. In Hilbert

spaces, i.e. complete metric space with said metric being induced by an inner product, these two operators act on vectors in the Hilbert space $\mathcal{H}$. There are many systems in which there exist such raising and lowering operators, but all (bosonic)[1] annihilation and creation operators must satisfy the following properties: for $\hat{a}, \hat{a}^* \in f : \mathcal{H} \to \mathcal{H}$

$$\begin{aligned} [\hat{a}, \hat{a}] = [\hat{a}^*, \hat{a}^*] = 0 \\ [\hat{a}, \hat{a}^*] = 1 \end{aligned} \tag{1}$$

Such an operator is useful in that given another operator of interest N, assuming that

$$[N, \hat{a}] = c\hat{a} \tag{2}$$

for some scalar c and given some eigenvector of N, $N|n\rangle = n|n\rangle$,

$$\begin{aligned} N\hat{a}|n\rangle &= (N\hat{a} + [N, \hat{a}])|n\rangle \\ &= \hat{a}n|n\rangle + c\hat{a}|N\rangle \\ &= (n + c)\hat{a}|n\rangle \end{aligned} \tag{3}$$

Creation operators have positive c, while annihilators have negative c. Furthermore, if N is a Hermitian operator (which many operators of interest, such as observables are), c is real and thus the hermitian conjugate of $\hat{a}$ is equal to $\hat{a}^*$, i.e.

$$[N, \hat{a}^*] = -c\hat{a}^* \tag{4}$$

When the corresponding operator to the annihilation and creation operators is the Hamiltonian, the state with the property of

$$\hat{a}|\psi_0\rangle = 0 \tag{5}$$

is labeled as the ground state.

From these commutation relations, we can prove that the ground state is the minimum uncertainty state.

Theorem 1 (Minimum uncertainty states). *For creation and annihilation operators $\hat{a}^*, a$ obeying the commutation relations $[\hat{a}, \hat{a}] = [\hat{a}^*, \hat{a}^*] = 0$, $[\hat{a}, \hat{a}^*] = 1$, The ground state $|\psi_0\rangle$ satisfying the relation $\hat{a}|\psi_0\rangle = 0$, and operators $\hat{x} = \hat{a} + \hat{a}^*, \hat{p} = -i(\hat{a} - \hat{a}^*)$, has a variance of x times variance of p is equal to 1.*

Proof.

$$\begin{aligned} \sigma_x^2 &= \langle x^2 \rangle - \langle x \rangle^2 \\ &= \langle \psi_0 | x^2 | \psi_0 \rangle + \langle \psi_0 | x | \psi_0 \rangle^2 \end{aligned} \tag{6}$$

[1] for fermions, replace the commutators with anti-commutators

but,

$$\begin{aligned}\langle\psi_0|\hat{x}|\psi_0\rangle^2 &= \langle\psi_0|(\hat{a}+\hat{a}^*)|\psi_0\rangle^2 \\ &= (\langle(\hat{a}^*)^*\psi_0|\psi_0\rangle + \langle\psi_0|\hat{a}\psi_0\rangle)^2 \\ &= 0^2\end{aligned} \tag{7}$$

so,

$$\begin{aligned}\sigma_x^2 &= \langle\psi_0|\hat{x}^2|\psi_0\rangle \\ &= \langle\psi_0|(\hat{a}^2+\hat{a}\hat{a}^*+\hat{a}^*\hat{a}+(\hat{a})^2)|\psi_0\rangle \\ &= 0+\langle\psi_0|\hat{a}\hat{a}^*|\psi_0\rangle+0+0\end{aligned} \tag{8}$$

for σ_p^2,

$$\begin{aligned}\sigma_p^2 &= \langle\hat{p}^2\rangle - \langle\hat{p}\rangle^2 \\ &= \langle\psi_0|\hat{p}^2|\psi_0\rangle + \langle\psi_0|\hat{p}|\psi_0\rangle^2\end{aligned} \tag{9}$$

but,

$$\begin{aligned}\langle\psi_0|\hat{p}|\psi_0\rangle^2 &= \langle\psi_0|(\hat{a}-\hat{a}^*)|\psi_0\rangle^2 \\ &= (-\langle(\hat{a}^*)^*\psi_0|\psi_0\rangle + \langle\psi_0|\hat{a}\psi_0\rangle)^2 \\ &= 0^2\end{aligned} \tag{10}$$

so,

$$\begin{aligned}\sigma_p^2 &= \langle\psi_0|\hat{p}^2|\psi_0\rangle \\ &= \langle\psi_0|-(-\hat{a}^2-\hat{a}\hat{a}^*+\hat{a}^*\hat{a}+(\hat{a}^*)^2)|\psi_0\rangle \\ &= 0+\langle\psi_0|\hat{a}\hat{a}^*|\psi_0\rangle+0+0\end{aligned} \tag{11}$$

and

$$\begin{aligned}\langle\psi_0|\hat{a}\hat{a}^*|\psi_0\rangle &= \langle\psi_0|[\hat{a},\hat{a}^*]-\hat{a}^*\hat{a}|\psi_0\rangle \\ &= \langle\psi_0|1|\psi_0\rangle \\ &= 1\end{aligned} \tag{12}$$

thus we see that

$$\sigma_x\sigma_p = 1 \tag{13}$$

□

As a specific example of annihilation and creation operators, consider the quantum harmonic oscillator. in this system, the creation and annihilation operators are defined as

$$\begin{aligned}\hat{a} &= \sqrt{\frac{m\omega}{2\hbar}}\left(\hat{x}+\frac{i}{m\omega}\hat{p}\right) \\ \hat{a}^* &= \sqrt{\frac{m\omega}{2\hbar}}\left(\hat{x}-\frac{i}{m\omega}\hat{p}\right)\end{aligned} \tag{14}$$

Note that redimentionalizing this argument for say $\hat{x}$ being the position operator and $\hat{p}$ being the momentum operator yields the familiar equation $\sigma_x \sigma_p = \hbar/2$, thus we see that the ground state is the minimal uncertainty state.

Another specific example is in the Fock space. The Fock space is a Hilbert space in which the states are representative of zero, one, two and so on particles. Such states can be written as $|0\rangle, |1\rangle, |2\rangle \ldots$. The annihilation and creation operators add and remove particles in such states respectively. Formally, a Fock space $F_+(H)$ can be defined as

$$\bigoplus_{n=0}^{\infty} \overline{S^* H^{\otimes n}} = \mathbb{C} \oplus H \oplus (S^*(H \otimes H)) \oplus (S^*(H \otimes H \otimes H)) \oplus \ldots \tag{15}$$

where S^* is the symmetrizing operator[2] and the overline represents closure. We can write the 0th term in the sum as $|0\rangle$, the first as $|1\rangle$, and so on, thus any state in $F_+(H)$ can be written as

$$|\psi\rangle = a_0|0\rangle \oplus \sum_i a_i|\psi_i\rangle \oplus \sum_{ij} a_{ij} S^*(|\psi_i\rangle \otimes |\psi_j\rangle) \oplus \ldots \tag{16}$$

such that $\langle\psi|\psi\rangle$ converges. As a shorthand, we write states that have n particles (element of $H^{\otimes n}$) as $|n_{k_1}, n_{k_2}, n_{k_3}, \ldots, n_{k_m}\rangle$ where $\sum n_{k_m} = n$. On this space, we can define creation operators as

$$\begin{aligned} \hat{a}^*_{k_i}|n_{k_1}, n_{k_2}, \ldots, n_{k_i}, \ldots, n_{k_m}\rangle &= \sqrt{n_{k_i}+1}|n_{k_1}, n_{k_2}, \ldots, n_{k_i}+1, \ldots, n_{k_m}\rangle \\ &\in H^{\otimes(n+1)} \end{aligned} \tag{17}$$

and annihlation operators as

$$\begin{aligned} \hat{a}_{k_i}|n_{k_1}, n_{k_2}, \ldots, n_{k_i}, \ldots, n_{k_m}\rangle &= \sqrt{n_{k_i}}|n_{k_1}, n_{k_2}, \ldots, n_{k_i}-1, \ldots, n_{k_m}\rangle \\ &\in H^{\otimes(n-1)}. \end{aligned} \tag{18}$$

The relation of a_{k_i} acting on a state where n_{k_i} is zero remains the same:

$$\hat{a}_{k_i}|n_{k_1}, n_{k_2}, \ldots, n_{k_i}=0, \ldots, n_{k_m}\rangle = 0. \tag{19}$$

We also see that the commutation relations of bosonic creation and annihilation operators are preserved:

$$\begin{aligned} [\hat{a}_i, \hat{a}^*_j] &= \delta_{ij} \\ [\hat{a}^*_i, \hat{a}^*_j] = [\hat{a}_i, \hat{a}_j] &= 0 \end{aligned} \tag{20}$$

[2]There is also the option for S^* to be replaced with $\wedge^*$, the antisymmetrizing operator for fermionic statistics.

From here we can define coherent states as eigenvectors of $\hat{a}_{k_i}, \hat{a}^*_{k_i}$. For $\alpha, i \in (\mathbb{Z} \geq 0)$,

$$|\alpha\rangle = e^{\frac{-|\alpha|^2}{2}} \sum_{n=0}^{\infty} \frac{\alpha^n}{\sqrt{n!}} |0, 0, \ldots, n_i, 0, \ldots) \tag{21}$$

are coherent states in the fock basis.

Using eq. 21, we see that another way to write coherent states is by acting on the ground state with operator $D(\alpha)$ called the *displacement operator* where

$$\hat{D}(\alpha) = e^{-\alpha \hat{a}^* - \alpha^* \hat{a}}. \tag{22}$$

A squeezed coherent state is another quantum state in which the wave function of the state has a standard deviation in one of the non-commuting operator's ground state below that of the ground state. In the case of the quantum harmonic oscillator, an example of a squeezed coherent state is one in which the standard deviation of x, Δx_{ψ_α} is less than that of the ground state's standard deviation in x, Δx_{ψ_0}. In return however, as the Heisenberg uncertainty principle must be obeyed, the non-commuting variable momentum (p)'s uncertainty must be greater than that of the ground state such that $\Delta x_{\psi_\alpha} \Delta p_{\psi_\alpha} = \hbar/2$.

The squeezed coherent state can be written as the coherent state in eq. 22 acted upon by the squeeze operator $S(\xi)$ where the squeeze operator is defined by

$$\hat{S}(\xi) = e^{\frac{1}{2}(\xi^* \hat{a}^2 - \xi (\hat{a}^*)^2)} \tag{23}$$

Thus a squeezed coherent state $\phi = |\alpha, \xi\rangle$ can be written as

$$|\alpha, \xi\rangle = \hat{S}(\xi)\hat{D}(\alpha)|0\rangle \tag{24}$$

We are now ready to prove the following theorem.

Theorem 2. *The state for any $\alpha, \xi \in \mathbb{C}$, $\xi = re^{i\theta}$, $|\alpha, \xi\rangle$ is a minimum uncertainty state.*

Proof. Using the property $e^{\hat{A}} \hat{B} e^{-\hat{A}} = \hat{B} + [\hat{A}, \hat{B}] + \frac{1}{2!}[\hat{A}, [\hat{A}, \hat{B}]] + \ldots$, the following equalities are true, all of which can be verified through calculation .

$$\hat{D}^*(\alpha)\hat{D}(\alpha) = 1 \tag{25}$$

$$\begin{aligned} \hat{D}^*(\alpha)\hat{a}\hat{D}(\alpha) &= \hat{a} + \alpha \\ \hat{D}(\alpha)\hat{a}\hat{D}^*(\alpha) &= \hat{a} - \alpha \end{aligned} \tag{26}$$

$$\hat{S}^*(\xi)\hat{S}(\xi) = \hat{S}(-\xi)\hat{S}(\xi) = 1 \tag{27}$$

$$\begin{aligned}\hat{S}^*(\xi)\hat{a}\hat{S}(\xi) &= \hat{a}\cosh r - \hat{a}^* e^{i\theta}\sinh r \\ \hat{S}(\xi)\hat{a}\hat{S}^*(\xi) &= \hat{a}^*\cosh r - \hat{a}e^{-i\theta}\sinh r\end{aligned} \tag{28}$$

Let us write $\hat{a} = A + i\lambda B$, $\lambda \in \mathbb{R}^3$.
Let us also call

$$\hat{C} = -i[\hat{A}, \hat{B}] \tag{29}$$

and

$$\hat{F} = \{\hat{A}, \hat{B}\} - 2\langle\hat{A}\rangle\langle\hat{B}\rangle. \tag{30}$$

Using $\hat{F}, \hat{C}$, we can rewrite the uncertainty relation as $(\Delta\hat{A})^2(\Delta\hat{B})^2 = \frac{1}{4}\left(\langle\hat{F}\rangle^2 + \langle\hat{C}\rangle^2\right)$.[4] Applying this formula to $\hat{a}$, we see

$$\begin{aligned}\Delta\hat{A}^2 &= \frac{1}{2}\left(\lambda_i\langle\hat{F}\rangle + \lambda_r\langle\hat{C}\rangle\right) \\ \Delta\hat{B}^2 &= \frac{1}{|\lambda|^2}\Delta\hat{A}^2 \\ \lambda_i\langle\hat{C}\rangle - \lambda_r\langle\hat{F}\rangle &= 0\end{aligned} \tag{31}$$

Multiplying we see our familiar uncertainty relation

$$\Delta\hat{A}^2\Delta\hat{B}^2 \geq \frac{1}{4}\left(\langle\hat{F}\rangle^2 + \langle\hat{C}\rangle^2\right) \tag{32}$$

□

2.2 Adiabatic Control

The adiabatic theorem is a fundamental concept in quantum mechanics that describes the behavior of a quantum system under a slowly changing external influence. It states that if a quantum system is subjected to a slow change in its Hamiltonian, and if the initial state of the system remains in the eigenstate of the Hamiltonian throughout this change, then the system will remain in an instantaneous eigenstate of the Hamiltonian throughout the process. The original statement as said by Max Born and Vladmir Fock is as follows: "A physical system remains in its instantaneous eigenstate if a given perturbation is acting on it slowly enough and if there is a gap between the eigenvalue and the rest of the Hamiltonian's spectrum"[6].

[3] This can be thought of breaking $\hat{a}$ into hermitian and anti-hermitian components. For our usual operators $\hat{q}, \hat{p}$, the hermitian component is $\hat{q}$ and the antihermitian is $\frac{\partial}{\partial x}$

[4] As a sanity check, our usual operators for position and momentum $\hat{q}, \hat{p}$ follow the commutation relation $[\hat{q}, \hat{p}] = i\hbar \implies (\Delta\hat{q})^2(\Delta\hat{p})^2 \geq \frac{\hbar^2}{4}$ following our formula.

Theorem 3 (Adiabatic Theorem). *Given a slowly changing hamiltonian $H(t)$ ($\dot{H}(t) = o(1)$) with instantaneous eigenstates $|n\rangle$ and distinct energies $E_n(t)$ ($E_n(t) \neq E_m(t)$ for $n \neq m$), the system evolves from the initial state*

$$|\psi(0)\rangle = \sum_n c_n(0)|n(0)\rangle \tag{33}$$

to time t

$$|\psi(t)\rangle = \sum_n c_n(t)|n(t)\rangle. \tag{34}$$

The coefficients follow the formula

$$c_n(t) = c_n(0)e^{i\theta_n(t)}e^{i\gamma_n(t)} + o(1) \tag{35}$$

where the dynamical phase θ_n is given by

$$\theta_n(t) = -\frac{1}{\hbar}\int_0^t E_n(t')dt' \tag{36}$$

and the geometric phase γ_n is given by

$$\gamma_n = i\int_0^t \langle n(t')|\dot{n}(t')\rangle dt'. \tag{37}$$

Proof. Given the time dependent schrödinger equation

$$i\hbar|\dot{\psi}(t)\rangle = H(t)|\psi(t)\rangle, \tag{38}$$

differentiate the left hand side to get

$$i\hbar|\dot{\psi}(t)\rangle = i\hbar\dot{c}_n(t)|n(t)\rangle + i\hbar\sum_n c_n(t)|\dot{n}(t)\rangle. \tag{39}$$

Then applying $\langle c_m(t)|$ to both sides of eq. 38

$$i\hbar\langle c_m(t)|\dot{\psi}(t)\rangle = i\hbar\dot{c}_m(t) + i\hbar\sum_n c_n(t)\langle m(t)|\dot{n}(t)\rangle = c_m(t)E_m(t). \tag{40}$$

But we can rewrite

$$\dot{H}(t)|n(t)\rangle + H(t)|\dot{n}(t)\rangle = \dot{E}_n(t)|n(t)\rangle + E_n(t)|\dot{n}(t)\rangle. \tag{41}$$

Also note for $m \neq n$

$$\langle m(t)|\dot{n}(t)\rangle = -\frac{\langle m(t)|\dot{H}(t)|n(t)\rangle}{E_m(t) - E_n(t)}. \tag{42}$$

Substituting into eq. 40 and rearranging constants we see,

$$\dot{c}_m(t) + \left(\frac{i}{\hbar}E_m(t) + \langle m(t)|\dot{m}(t)\rangle\right)c_m(t) = \sum_{n\neq m}\frac{\langle m(t)|\dot{H}(t)|n(t)\rangle}{E_m(t) - E_n(t)}c_n. \tag{43}$$

but since $E_m(t) - E_n(t) \neq 0$ and $\dot{H}(t) \sim 0$, eq. 43 is on order $o(1)$. (this is called the adiabatic approximation)

Solving the differential equation

$$\dot{c}_m(t) = i\left(-\frac{E_m(t)}{\hbar} + i\langle m(t)|\dot{m}(t)\rangle\right)c_m(t) + o(1) \tag{44}$$

by integrating results in

$$c_m(t) = c_n(0)e^{i\theta_n(t)}e^{i\gamma_n(t)} + o(1). \tag{45}$$

□

2.3 Hyperbolic Geometry

This section[5] could start from the half plane representation of hyperbolic geometry, but it seems that perhaps starting from an extrinsic definition, similar to how spherical geometry is often introduced, could be more enlightening.

Thus, let us start with constructing an object with constant negative curvature (the defining characteristic of hyperbolic geometry, in contrast to positive curvature in spherical geometry). As $\mathbb{S}^2$ is often defined as a surface is embedded in 3 dimensions, we will do similarly here. We will also come to see that it is impossible to preserve the negative curvature and fully immerse the surface in $\mathbb{R}^3$[6].

To define this surface, we must first discuss the object called the "tractrix". The tractrix can be defined on a 2d plane by the parametrized path. Starting at in the Cartesian plane, $(R, 0) \in \mathbb{R}^2$, following the differential equation

$$\frac{dr}{d\sigma} = -\frac{r}{R}, r = Re^{\frac{-\sigma}{R}} \tag{46}$$

where r is the distance to the y axis, and σ is arc length along the tractrix. Explicitly, the curve comes out to be

$$y = r\,\text{arsech}\left(\frac{x}{R}\right) - \sqrt{R^2 - x^2} \tag{47}$$

The pseudosphere is defined as the surface created by revolving a tractrix about its asymptote, $x = 0$. See fig. 1a.

The gaussian curvature of the pseudosphere is a constant $-\frac{1}{R^2}$. A geometric proof of this statement is found in [12] chapter 6.3.

Note that lines in hyperbolic geometry should extend infinitely in any direction, but the lines on the pseudospheres end along the and of the tractrix

[5] I will assume in this section that a basic knowledge of spherical geometry is understood as it is perhaps the more common form of non-euclidan geometry

[6] For the full proof, see [9]

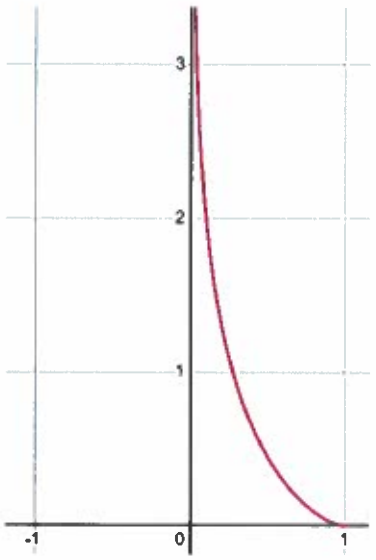

(a) Graph of the tractrix

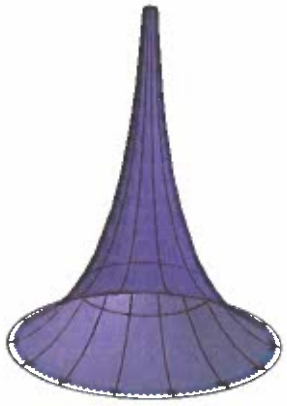

(b) Image of pseudosphere generated by revolving the tractrix along the asymptote

Figure 1: visualizations of the pseudosphere

or they loop back on themself.[7] This suggests that the while the pseudosphere has constant negative curvature, it is not am embedding of thw entire hyperbolic plane. To understand the whole hyperbolic plane, we have to map the whole plane somehow to $\mathbb{R}^n$. to do so, we will consider a conformal map of the pseudosphere onto $\mathbb{R}^2$, but the metric will no longer be the euclidean one.

The Beltrami half-plane model (also known as the Poincaré half-plane model) is a representation of the hyperbolic plane. The plane denoted $\mathbb{H}^2$ is given the metric of

$$ds^2 = \frac{dx^2 + dy^2}{y^2} \tag{48}$$

We will take our coordinates on the half plane to be the complex numbers. To see how this model relates to the pseudosphere, the pseudosphere can be conformally mapped to the region $x \in [0, 2\pi)$ and $y > 1$.

Now that we have a representation of the hyperbolic plane, let us examine the geodesics on the half plane representation.

Theorem 4. *The straight hyperbolic lines (h-lines) on $\mathbb{H}^2$ are either vertical lines, or half circles perpendicular to the x-axis.*

[7]Intuitively, the pseudosphere has no more "space" to expand into past y=0. The euclidean metric in $\mathbb{R}^3$ does not "expand" fast enough to embed the whole hyperbolic plane.

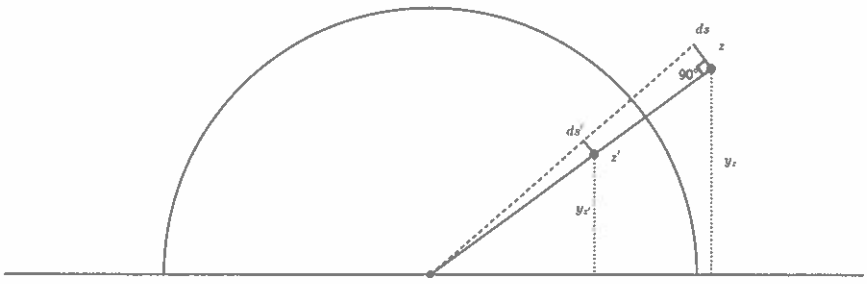

Figure 2: visual proof of inversion across circles centered on x-axis preserving distances

Proof sketch: The straight h-line connecting two points with the same x coordinate must be a straight vertical euclidean line since any deviation in the x means dx^2 is positive thus causing ds^2 to be larger.

To see the straight h-lines connecting two points that do not have the same x coordinate lies on the circle perpendicular to the x-axis and intersects the two points, we need to show that inversions across circles centered along the x-axis sends h-lines to h-lines.

Consider any circle c centered on the x-axis. Then consider any point z in the half plane and its inversion across c. We want to show any ds emanating off of the point z remains the same length after its inversion across c. Since the inversion is anti-conformal, angles are preserved (up to a negative sign), thus showing one ds_0 emanating off of z's distance is preserved implies all ds emanating off of z has their distances preserved.

Consider figure. 2. the distance element ds is perpendicular to the radius of the circle starting at the point z. The inversion of z and ds are z' and ds'. Smaller ds makes the angle between the radius and ds' approach a right angle. We can also see that

$$d_h s' = \frac{ds'}{y'_z} = \frac{ds}{y_z} = d_h s \tag{49}$$

where $d_h()$ is the hyperbolic length and $d()$ is the euclidean length.

Now consider figure 3. The points along the purple arc ab reflect to the points on the vertical line $a'b'$. Since the line $a'b'$ is a h-line, the purple arc must also be the line that minimizes distance between ab.

□

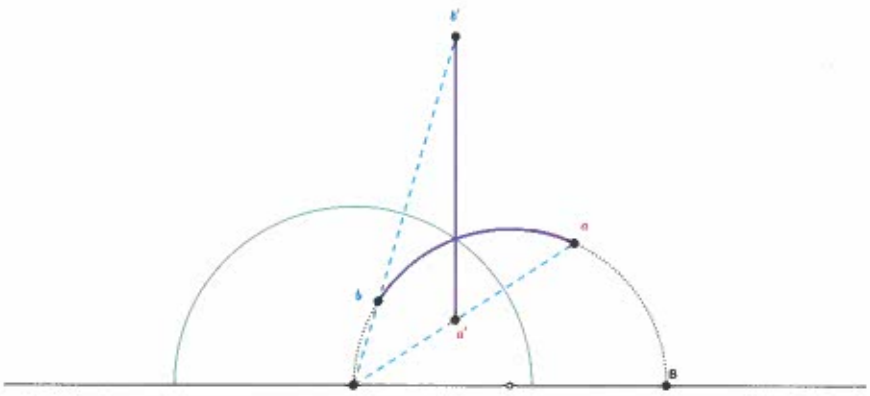

Figure 3: visual proof of unique circular arc connecting a, b inverting to straight line

Taking the upper half plane and applying the transformation [8]

$$f(z) = \frac{iz+1}{z+i} \tag{50}$$

gives the half plane model. This transformation maps the x-axis to the unit circle, and the entire half plane inside the unit disk.

The resulting metric in the Poincaré disk is $d\hat{s}$

$$d\hat{s} = \frac{1}{1-|z|^2} ds \tag{51}$$

It is clear to see that the euclidean circle centered at the origin on the Poincaré disk is also a hyperbolic circle (h-circle). We will see later in the Möbius transform section that Möbius transformations preserve circles on the Poincaré disk. Combined with the fact that Möbius transformations that preserve the unit disk are isometries in the Poincaré disk (see [11]), we see that euclidean circles are h-circles in the Poincaré disk, as well as in the half plane model.

While euclidean circles are in fact h-circles as well, they do not share the same center. The formula for the center of the h-circle given its euclidean center is given by the formula

$$x + iy \mapsto x + iy\cosh\rho \tag{52}$$

where ρ is the euclidean radius.

[8] This transformation is a Möbius transformation, discussed in section 2.4.

The further down the euclidean circle is, the closer the hyperbolic center is to the bottom edge of the circle. The limit where the hyperbolic center is touching the circle happens at the x-axis. These objects in hyperbolic space are called *horocycles*.

2.4 Möbius Transformations

We provide an overview of Möbius transformations, see, for example, [12]. A Möbius transformation is a mapping $f : \mathbb{C} \to \mathbb{C}$ of the form

$$f(z) = \frac{az + b}{cz + d}$$

for $a, b, c, d \in \mathbb{C}$.

All Möbius transformations of the above form can be written as a composition of 4 transformations.

$$\begin{aligned} z &\mapsto z + \frac{d}{c} \\ z &\mapsto \frac{1}{z} \\ z &\mapsto -\frac{ab - dc}{c^2} z \\ z &\mapsto z + \frac{a}{c} \end{aligned} \tag{53}$$

Each one of these preserves circles (assuming straight lines are circles with infinite radius), thus the whole transformation preserves circles.

We write the matrix $[f]$ associated with f as

$$[f] = \begin{bmatrix} a & b \\ c & d \end{bmatrix}.$$

The mapping $f \to [f]$ is a group homomorphism.

A non-identity Möbius transformation has two fixed points, counted with multiplicity, given by

$$\xi_{\pm} = \frac{(a - d) \pm \sqrt{(a - d)^2 + 4bc}}{2c}. \tag{54}$$

We use the same letter as in Eq. (66) since the points $\xi_{\pm}$ in Eq. (66) will be fixed points of a specific Möbius transformation.

The discriminant in eq. 66 determines the number of fixed points, and the type of Möbius transformation. Letting $\Delta = (a - d)^2 + 4bc$, if $\Delta = 0$, the transformation is *parabolic*. If $\Delta < 0$, the transformation is *loxodromic*[9].

[9] We will not be using this transformation further

Finally, if $\Delta > 0$, the transformation is either *hyperbolic* or *elliptic*. To conceptually distinguish the difference between the final two cases, it is easiest to break up the Möbius transformation.

Let M be any Möbius transformation. We will use a decomposition

$$M = S \circ T \circ S^{-1}$$

with S given by

$$S = \frac{z - \xi_-}{z - \xi_+} \tag{55}$$

in the elliptic and hyperbolic cases, and

$$S = \frac{1}{z - \xi_\pm} \tag{56}$$

in the parabolic case. The transformation T is a rotation $z \mapsto e^{i\theta}z$ in the elliptic case, a translation $z \mapsto z + \beta$ in the parabolic case, and a dilation $z \mapsto rz$ in the hyperbolic case for some non-zero $\theta, r \in \mathbb{R}$ and $\beta \in \mathbb{C}$. The compositions $S \circ M = T \circ S$ give the normal form of M.

In this paper, we only consider Möbius transformations that preserve the open unit disk D. This is the case if and only if the transformation takes the form

$$M(z) = \frac{az + b}{\bar{b}z + \bar{a}} \tag{57}$$

for some $a, b \in \mathbb{C}$ with $|a| > |b|$. There are three classes of such transformations: elliptic, parabolic, and hyperbolic. The positions of the fixed points $\xi_\pm$ determine the class. An automorphism of D is

i) elliptic if $\xi_- \neq \xi_+$ and only one fixed point is in D, in which case the points are related by circle inversion, i.e. $\xi_+ = 1/\overline{\xi_-}$,

ii) parabolic if there is a single fixed point $\xi_- = \xi_+$ on the unit circle, and

iii) hyperbolic if $\xi_- \neq \xi_+$ and both fixed points are on the unit circle.

Alternatively, we can also consider the transformation more geometrically as

$$M' = J \circ T' \circ J \tag{58}$$

where

$$J(z) = \frac{R^2}{\bar{z} - \bar{q}} + q \tag{59}$$

is inversion in the circle centered at q with radius R, with q and R to be specified, and T' is a Euclidean similarity transformation specific to each type of automorphism: i) In the elliptic case, T' is a rotation; ii) In the hyperbolic case T' is a translation; iii) In the parabolic case, T' is a dilation.

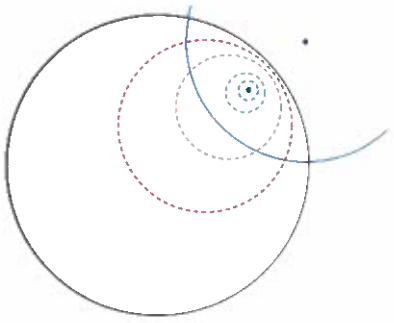

(a) Sample paths in elliptic case

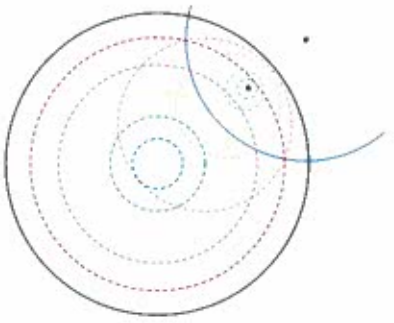

(b) Sample paths and inversions J of sample paths over the magenta circle

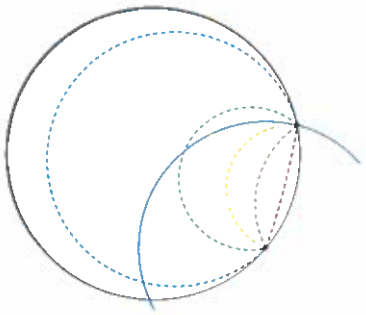

(c) Sample paths in hyperbolic case

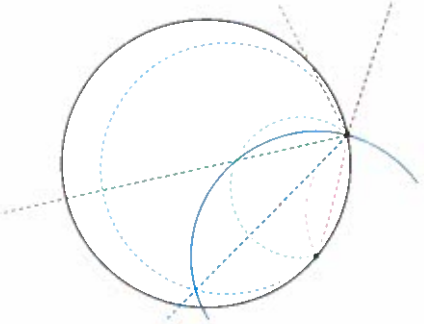

(d) Sample hyperbolic cases and inversions J of sample paths over the magenta circle

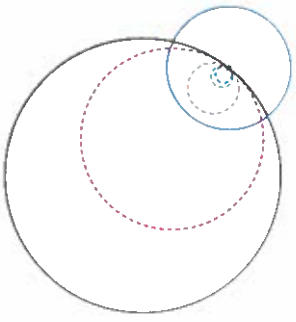

(e) Sample paths in parabolic case

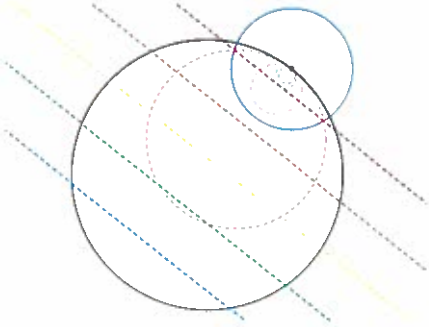

(f) Sample parabolic cases and inversions J of sample paths over the magenta circle

Figure 4: Decompositions of different hyperbolic motions; The reflections J are described as reflections along the solid magenta circles. The dashed rainbow lines in the first column represent different possible paths before reflection J and the reflections of such paths are depicted as the thicker dotted lines with the same respective color the second column.

Corresponding to this, we will sometimes call the case i) hyperbolic rotation, ii) hyperbolic dilation and iii) hyperbolic translation.

In the elliptic case, J is inversion in the circle centered at the exterior fixed point and orthogonal to the boundary. The transformation T' is the rotation

$$T'(z) = ze^{is} \tag{60}$$

for some $s \in \mathbb{R}$. Figures 4a, and 4b illustrate this process.

In the hyperbolic case, J is inversion in the circle of arbitrary radius centered at the single fixed point $\xi = \xi_{\pm}$, and T' is the translation

$$T'(z) = z + is\xi. \tag{61}$$

Figures 4c, and 4d illustrate this process.

In the parabolic case, J is inversion in the circle centered at ξ_+ passing through ξ_-, and T' is the dilation

$$T'(z) = s(z - \xi_-) + \xi_-. \tag{62}$$

Figures 4e, and 4f illustrate this process.

The invariant curves of elliptic, parabolic, and hyperbolic automorphisms are hyperbolic circles, horocycles, and hypercycles respectively. These curves are Euclidean circles or circular arcs in D. In the Poincaré disk model, a Euclidean circle corresponds to

i) a hyperbolic circle if it is contained within D,

ii) a horocycle if it is tangent to the unit circle,

iii) a hypercycle if it intersects the unit circle at two points at non-right angles, and

iv) a hyperbolic line if it intersects the unit circle orthogonally.

3 Setup and results

We consider the family of quadratic Hamiltonians parameterized by $\omega \geq 0$ and $\alpha \in \mathbb{C}$ given by

$$H = \omega a^* a + \frac{\alpha}{2} a^2 + \frac{\bar{\alpha}}{2} a^{*2}. \tag{63}$$

The operators a, a^* are irreducible representations of the canonical commutation relation $[a, a^*] = 1$. Our results will be independent of a choice of representation. A *squeezed state* ψ is a state satisfying

$$(a + za^*)\psi = 0 \tag{64}$$

for some $z \in \mathbb{C}$. The state ψ exists if and only if $|z| < 1$, in which case it is determined up to a phase by z. In the Schrödinger representation, solutions of the equation are multiples of

$$\psi(x) = \mathrm{e}^{-\frac{1+z}{1-z}\frac{x^2}{2}}.$$

The solutions are indeed in $L^2(\mathbb{R})$ if and only if the condition $|z| < 1$ holds, see [3].

We will use $[\psi(z)]$ to denote the complex line spanned by solutions of Eq. (64) and by $\psi(z)$ or $|\psi(z)\rangle$ a vector in $[\psi(z)]$ of unit norm. The manifold

$$\mathcal{C} := \{[\psi(z)], |z| < 1\}$$

of the complex projective space of $\mathcal{H}$ is formed by the set of all squeezed states. The mapping

$$\begin{aligned} F : D &\to \mathcal{C} \\ z &\mapsto [\psi(z)] \end{aligned}$$

associating a point in the open unit disk $D \subset \mathbb{C}$ with the squeezed state $[\psi(z)]$ is one-to-one.

The disk D equipped with distance

$$d(z, w) = \ln \frac{|\bar{z}w - 1| + |z - w|}{|\bar{z}w - 1| - |z - w|}$$

is known as the Poincaré disk model of hyperbolic geometry. In particular, the hyperbolic distance from a point z to the origin is

$$d(0, z) = \ln \frac{1 + |z|}{1 - |z|}. \tag{65}$$

The Poincaré metric, the metric induced by d_h, is

$$g_h = 4\frac{1}{(1 - |z|^2)^2}|dz|^2.$$

In Section 2.4 we will discuss the Poincaré disk model in more detail. In particular, we will introduce motions of the Poincaré disk and their invariants: hyperbolic circles, horocycles and hypercycles.

Our main focus is on the pullback of dynamics generated by H on the Poincaré disk. The qualitative properties of the dynamics depend on the spectral properties of the Hamiltonian in Eq. (63). There are three cases that we express in terms of parameters ω, α.

i) The *stable case:* If $\omega > |\alpha|$, then the Hamiltonian has the pure point spectrum $\sigma = \lambda\left(n + \frac{1}{2}\right) - \frac{\omega}{2} \quad (n = 0, 1, 2, \ldots)$.

ii) The *free case:* If $\omega = |\alpha|$, then the Hamiltonian has the absolutely continuous spectrum $\sigma = [-\omega, \infty)$.

iii) The *unstable case:* If $\omega < |\alpha|$, then the spectrum is $(-\infty, \infty)$.

Let $\lambda = \sqrt{\omega^2 - |\alpha|^2}$. The complex points

$$\xi_\pm = \frac{\omega \pm \lambda}{\alpha} \tag{66}$$

will play an important part in describing the dynamics of the evolution $U(t) = \mathrm{e}^{-itH}$ generated by the Hamiltonian in Eq. (63). In the stable case, $\xi_- \in D$ represents the ground state of H and $\xi_+ \notin D$. In the free and unstable cases, we have $|\xi_\pm| = 1$, where the points are degenerate in the free case. We will show in Section 4 that the evolution $U(t)$ leaves the manifold of squeezed states $\mathcal{C}$ invariant. The pullback of $U(t)$ gives a motion $M(t)$ of the Poincaré disk. Explicitly,

$$M(t)z = F^{-1}\left([U(t)\psi(z)]\right). \tag{67}$$

We write $z(t) = M(t)z$. By the above, $z(t)$ satisfies $[U(t)\psi(z)] = [\psi(z(t))]$. We now describe the geometry of the motion.

Theorem 5. *Let $C = \{z(t) | t \in [-\infty, \infty)\}$. Then*

i) The stable case: C is a hyperbolic circle with center ξ_- (Fig. 5a).

ii) The free case: C is a horocycle tangent to the unit circle at the point $\xi_- = \xi_+$ (Fig. 5b).

iii) The unstable case: C is a hypercycle intersecting the unit circle at the points $\xi_\pm$ (Fig. 5c).

In cases i) and ii), the motion is clockwise, and in case iii) the trajectory travels from ξ_- to ξ_+.

The proof of this theorem and more details about the motion are in Section 4.

In Section 5, we will discuss several control problems. In particular, we derive the set of states reachable by a sequence of pulses obtained by switching n times between two quadratic Hamiltonians H_0, H_1.

Finally, in Appendix A we show that the manifold of squeezed states $\mathcal{C}$ equipped with the Fubini-Study metric is a realization of hyperbolic geometry.

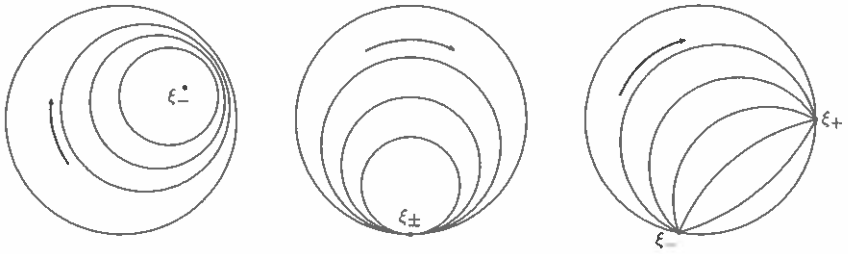

(a) Stable case (b) Free case (c) Unstable case

Figure 5: Trajectories of $z(t)$.

4 Motions of squeezed states

In this section, we prove Theorem 5. We start by showing that $U(t) = e^{-itH}$ indeed preserves the unit disk and give an explicit formula for the corresponding Möbius transformation $M(t)$ in Eq. (67).

The evolution $U(t)$ generated by the Hamiltonian (63) preserves the linear space spanned by a, a^*. Let $a(t) = U^*(t)aU(t)$ be the Heisenberg evolution of a. Taking the time derivative and using $[H, a] = -\omega a - \bar{\alpha}a^*$, we get a system of equations

$$\begin{bmatrix} \dot{a}(t) \\ \dot{a}^*(t) \end{bmatrix} = i \begin{bmatrix} -\omega & -\bar{\alpha} \\ \alpha & \omega \end{bmatrix} \begin{bmatrix} a(t) \\ a^*(t) \end{bmatrix}. \tag{68}$$

The solution with $a(0) = a$ and $a^*(0) = a^*$ is $a(t) = u(t)a + v(t)a^*$, where $u(t), v(t)$ are complex functions whose form will be discussed later. This implies that for any complex function $z(t)$,

$$U^*(t)(a + z(t)a^*)U(t)\psi(z) = \Big((u(t) + z(t)\overline{v(t)})a + (v(t) + z(t)\overline{u(t)})a^*\Big)\,\psi(z).$$

We now pick the function $z(t)$ so that the combination of a, a^* on the right hand side annihilates $\psi(z)$, i.e.

$$\frac{v(t) + z(t)\overline{u(t)}}{u(t) + z(t)\overline{v(t)}} = z,$$

and conclude that $(a + z(t)a^*)U(t)\psi(z) = 0$. Explicitly, we showed that

$$[U(t)\psi(z)] = \psi(z(t)),$$

with

$$z(t) = \frac{zu(t) - v(t)}{-z\overline{v(t)} + \overline{u(t)}}.$$

Since $U(t)$ is unitary, $\psi(z(t))$ is in $L^2(\mathbb{R})$, so $|z(t)| < 1$ and the Möbius transformation $M(t) : z \to z(t)$ preserves the Poincaré disk. We will also check this explicitly after computing $u(t), v(t)$.

The Hamiltonian evolution $U(t)$ forms a group and hence the pullback $M(t) = F^{-1}U(t)$ is also a group, where

$$M(s) \circ M(t) = M(s+t), \quad s, t \in \mathbb{R}.$$

It follows that the fixed points of the Möbius transformations $M(s)$ are independent of s.

We now discuss the mapping $M(t)$ in each of the three cases.

4.1 The stable case

Let $\lambda = \sqrt{\omega^2 - |\alpha|^2}$. The solution of the system of equations (68) is

$$\begin{bmatrix} a(t) \\ a^*(t) \end{bmatrix} = \frac{a(\omega - \lambda) + \bar{\alpha}a^*}{2\lambda} e^{i\lambda t} \begin{bmatrix} -1 \\ \frac{\omega+\lambda}{\bar{\alpha}} \end{bmatrix} + \frac{a(\omega + \lambda) + \bar{\alpha}a^*}{2\lambda} e^{-i\lambda t} \begin{bmatrix} 1 \\ \frac{\lambda-\omega}{\bar{\alpha}} \end{bmatrix}.$$

This implies that

$$z(t) = \frac{\bar{\alpha}(e^{i\lambda t} - e^{-i\lambda t}) + z((\lambda - \omega)e^{i\lambda t} + (\omega + \lambda)e^{-i\lambda t})}{-\alpha z(e^{i\lambda t} - e^{-i\lambda t}) + ((\lambda - \omega)e^{-i\lambda t} + (\omega + \lambda)e^{i\lambda t})}.$$

The fixed points are then, c.f. Eq. (54),

$$\xi_\pm = \frac{\omega \pm \lambda}{\alpha}.$$

Since there are two distinct fixed points $\xi_\pm$ which are circle inversions of one another, the transformation $M(t)$ is elliptic. We have the decomposition

$$z(t) = (S \circ T \circ S^{-1})z \tag{69}$$

where S is given by Eq. (55) and T is the rotation $z \mapsto e^{-2i\lambda t}z$. This implies that $C = \{z(t) | t \in [-\infty, \infty)\}$ is a hyperbolic circle centered at ξ_-, with $\psi(\xi_-)$ being the ground state of H. The trajectory of $z(t)$ makes a full revolution in time π/λ.

4.2 The free case

The solution of the system of equations (68) gives

$$z(t) = \frac{-i\bar{\alpha}t - (1 - i\omega t)z}{i\alpha t z - (1 + i\omega t)}$$

which has a single fixed point

$$\xi = \frac{\omega}{\alpha}.$$

This is a parabolic transformation and its decomposition (69) can be written by taking S as defined in Eq. (55) and T to be the translation $z \mapsto z - i\alpha t$.

This shows that $C = \{z(t) | t \in [-\infty, \infty)\}$ is a horocycle touching the unit circle at ξ.

4.3 The unstable case

Let $\gamma = \sqrt{|\alpha|^2 - \omega^2}$. The solution of the system of equations (68) is

$$z(t) = \frac{-\bar{\alpha}(e^{\gamma t} - e^{-\gamma t}) + z((\omega + i\gamma)e^{\gamma t} - (\omega - i\gamma)e^{-\gamma t})}{\alpha z(e^{\gamma t} - e^{-\gamma t}) - ((\omega - i\gamma)e^{\gamma t} - (\omega + i\gamma)e^{-\gamma t})}$$

with fixed points

$$\xi_{\pm} = \frac{\omega \pm i\gamma}{\alpha}, \tag{70}$$

where $z(t) \to \xi_{\pm}$ as $t \to \pm\infty$. The fixed points lie on the unit circle so this is a hyperbolic transformation whose decomposition (69) is given by taking S as defined in Eq. (56) and T to be the dilation $z \mapsto e^{2\gamma t}z$.

This shows that $C = \{z(t) | t \in [-\infty, \infty)\}$ is a hypercycle connecting ξ_- to ξ_+.

5 Applications to control theory

The questions we study are motivated by [13] that studied reachable set in a similar control problem. Our methods allows us to give a full geometric characterization of reachable sets in several control problems associated with squeezed states.

5.1 Bang-bang control

We consider two quadratic Hamiltonians H_0, H_1 and the control sequence given by

$$\psi(t) = S_n \cdots S_j \cdots S_2 S_1 \psi(0) \tag{71}$$

where each operator S_j acts over a time interval of length Δt_j. Alternating between the time evolution operators corresponding to H_0 and H_1, we have

$$S_j = \begin{cases} e^{-iH_0\Delta t_j} & \text{for } j = 2k+1, \\ e^{-iH_1\Delta t_j} & \text{for } j = 2k, \end{cases}$$

and $t = \Delta t_1 + \Delta t_2 + \cdots + \Delta t_n$. The operator U_k is defined as the product

$$U_k = S_k \cdots S_2 S_1.$$

The control problem we consider involves evolving an initial squeezed state $[\psi(z_0)]$ into the target state $[\psi(z_f)]$ for given z_0 and z_f using bang-bang control (71). We consider several cases of H_0, H_1.

5.1.1 The stable case

We consider two stable Hamiltonians, i.e. $\omega > |\alpha|$,

$$H_0 = \omega a^* a,$$
$$H_1 = \omega a^* a + \frac{\alpha}{2} a^2 + \frac{\bar{\alpha}}{2} a^{*2},$$

where, for simplicity, we have chosen H_0 to be the standard harmonic oscillator. We are specifically interested in finding the minimum number of times that we need to use the Hamiltonian H_1 in order to move the initial state into the target state with complete freedom to pick Δt_j. Taking $n = 2k+1$, we want to find minimal n for which there exists a sequence $\Delta t_1, \ldots, \Delta t_n$ that solves the control problem. The answer depends only on the modulus of z_0 and z_f. Let ξ denote the fixed point in D associated with H_1. We define sequences R_{2k+1}, r_{2k+1} recursively as

$$R_{2k+1} = \frac{(1+|\xi|^2)R_{2k-1} + 2|\xi|}{2|\xi|R_{2k-1} + (1+|\xi|^2)}, \quad R_1 = |z_0|, \tag{72}$$

and

$$r_{2k+1} = \begin{cases} \frac{(1+|\xi|^2)r_{2k-1} - 2|\xi|}{-2|\xi|r_{2k-1} + (1+|\xi|^2)}, & \text{if } r_{2k-1} > \frac{2|\xi|}{1+|\xi|^2} \\ 0, & \text{otherwise.} \end{cases}, \quad r_1 = |z_0|. \tag{73}$$

Theorem 6. *The control problem* $[\psi(z_f)] = [U_{2k+1}\psi(z_0)]$ *has a solution if and only if*

$$r_{2k+1} \leq |z_f| \leq R_{2k+1}.$$

Proof. Using the mapping of squeezed states to the Poincaré disk, the problem is equivalent to the study of motions $F^{-1} \circ U_k$ on the disk. By Theorem 5, the trajectories $F^{-1} \circ S_k$ correspond to circles centered at the origin for odd terms and hyperbolic circles with hyperbolic center ξ for even terms. Thus for each S_{2k+1}, there is some maximum and minimum $|z|$-value reachable by that step, which we denote R_{2k+1} and r_{2k+1} respectively, see Fig. 6.

The initial terms are given by $R_1 = r_1 = |z_0|$. Subsequent terms are computed as follows: Given a Euclidean circle of radius R_{2k-1}, the next term R_{2k+1} is determined by the point on the circle with maximal hyperbolic distance from ξ, which is $p = -R_{2k-1}\xi/|\xi|$. Let q be the point antipodal to p on the hyperbolic circle centered at ξ passing through p. Then $R_{2k+1} = |q|$, which can be computed by converting the hyperbolic distance $d(0,q) = d(0,\xi) + d(p,\xi)$ to Euclidean distance using Eq. (65). We obtain the recursion Eq. (72).

For the minimal reachable radius, we get Eq. (73) using similar geometric considerations as for the maximal radius. The recursion holds as long as the the trajectory does not intersect with the hyperbolic circle centered at ξ passing through the origin. Once these intersect, the origin is reachable so the following term is zero. □

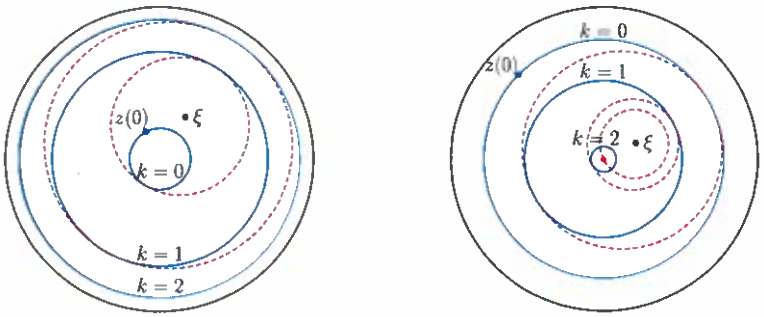

Figure 6: Illustrations of how to reach the maximum radius (left) and minimum radius (right).

Remark 1. *The recurrence equation for the maximum radius, Eq. (72), is a hyperbolic Möbius transformation* $R_{2k+1} = M(R_{2k-1})$ *with an explicit formula* $R_{2k+1} = M^{\circ k} R_1$ *and a corresponding matrix*

$$[M] = \begin{bmatrix} 1+|\xi|^2 & 2|\xi| \\ 2|\xi| & 1+|\xi|^2 \end{bmatrix}.$$

We can diagonalize $[M]$ *with*

$$U = \frac{1}{\sqrt{2}} \begin{bmatrix} 1 & 1 \\ 1 & -1 \end{bmatrix}, \quad D = \begin{bmatrix} (1+|\xi|)^2 & 0 \\ 0 & (1-|\xi|)^2 \end{bmatrix}.$$

Using $[M] = UDU^{-1}$ *and* $[M^{\circ k}] = UD^kU^{-1}$, *we have*

$$R_{2k+1} = \frac{(1+\Delta^{2k})R_1 + 1 - \Delta^{2k}}{(1-\Delta^{2k})R_1 + 1 + \Delta^{2k}}, \quad \Delta = \frac{1-|\xi|}{1+|\xi|}.$$

For large k, $\Delta^{2k} << 1$ *and we get an asymptotic formula*

$$1 - R_{2k+1} \approx 2\left(\frac{1-R_1}{1+R_1}\right)\Delta^{2k}.$$

5.1.2 The free case

Consider the Hamiltonians H_0, H_1 given by

$$H_i = \omega_i a^* a + \frac{\alpha_i}{2} a^2 + \frac{\bar{\alpha}_i}{2} a^{*2}$$

where $\omega_i = |\alpha_i|$ and the fixed points are $\xi_i = \omega_i/\alpha_i$. In order to describe the set of reachable states, we use arc-polygons, i.e. polygons whose edges are Euclidean circular arcs.

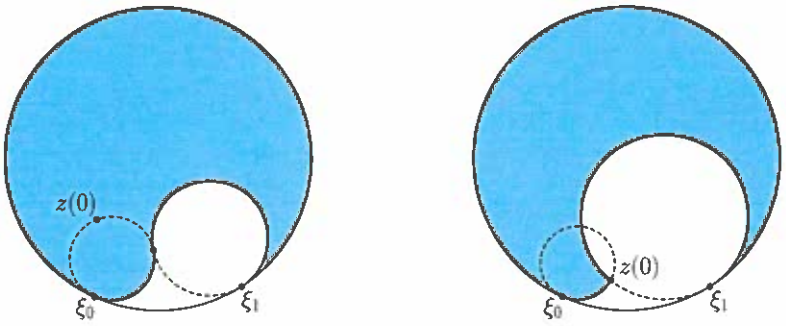

Figure 7: Set of reachable states (blue) in the free case after applying H_0, H_1.

Evolving some initial point z_0 under H_0 results in a trajectory along a horocycle through ξ_0. Applying H_1 then extends the reachable set to an arc-triangle (Fig. 7). In all cases, we have that

- ξ_0 is a vertex with internal angle π,
- ξ_1 is a vertex with internal angle zero, and
- the arc of the unit circle traversed clockwise from ξ_0 to ξ_1 is an edge.

The remaining vertex and edges are determined by the point where the horocycle through $z(0)$ and ξ_0 intersects with the horocycle through ξ_1 tangent to it. If the intersection point can be reached by evolving $z(0)$ under H_0, then the intersection point is the third vertex. Otherwise, the third vertex is $z(0)$. The remaining two edges are given by horocycle arcs connecting the third vertex to ξ_0 and ξ_1. The entire open disk is reachable with the sequence H_0, H_1, H_0.

5.1.3 The unstable case

For Hamiltonians H_0, H_1 where $\omega_i < |\alpha_i|$, the entire disk is reachable only when pairs of fixed points do not overlap (Fig. 8a), in which case any point in D can be reached with the sequence H_0, H_1, H_0. Otherwise, the final set is given by some arc-polygon with vertices $z(0)$, ξ_+^0, and ξ_+^1 (Fig. 8b).

The selection of H_0, H_1 that we present here does not encompass all cases, but we hope it convinces the reader that the geometric map gives a versatile method to think about control problems with squeezed states.

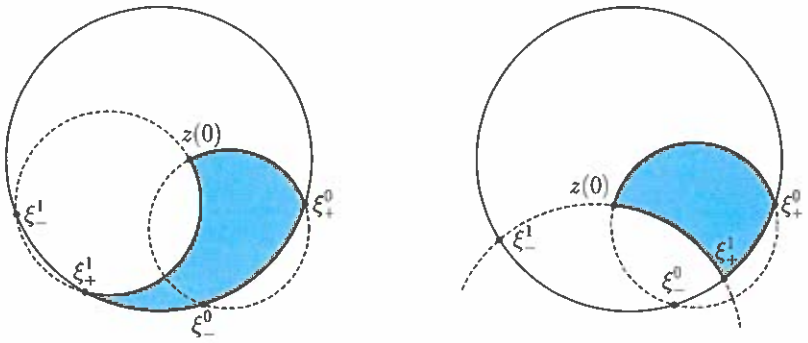

(a) Non-overlapping pairs of fixed points (b) Overlapping pairs of fixed points

Figure 8: Set of reachable states (blue) in the unstable case after applying H_0, H_1.

5.2 Adiabatic control

Provided $\omega^2 > |\alpha|^2$, the stable case, the Hamiltonian $H = H(\omega, \alpha)$ in Eq.(63) has a discrete spectrum with ground state $[\psi(\xi_-)]$. Recall that

$$\xi_\pm = \frac{\omega \pm \sqrt{\omega^2 - |\alpha|^2}}{\alpha}$$

are the fixed points of the motion of the Poincaré disk generated by the Hamiltonian.

We consider the family of Hamiltonians $H(t)$ corresponding to parameters $\omega(t), \alpha(t)$ that depend smoothly on $t \in [0, 1]$. Let $U_\epsilon(t)$ be the unitary generated by the slowly driven Schrödinger equation

$$\epsilon \dot{U}(t) = H(t)U(t), \quad U(0) = \mathbf{1}.$$

We assume that the parameters satisfy the constraint $\omega(t)^2 > |\alpha(t)|^2$. The ground state $[\psi(\xi_-(t))]$ of $H(t)$ is then protected by a gap, and a basic result of adiabatic theory [6, 10] gives the limit

$$\lim_{\epsilon \to 0} [U_\epsilon(t)\psi(\xi_-(0))] = [\psi(\xi_-(t))].$$

For the motion $M_\epsilon(t) = F^{-1} \circ U_\epsilon(t)$ on the Poincaré disk, this implies that

$$\lim_{\epsilon \to 0} M_\epsilon(t)\xi_-(0) = \xi_-(t).$$

The idea of adiabatic control theory is to move the initial state $[\psi(\xi_-(0))]$ into the target state $[\psi(\xi_-(t))]$ by slowly changing the corresponding Hamiltonian $H(t)$. In the limit of infinitely slow driving, the motion traces the

curve $\xi_-(t)$ on the disk. Our goal is to describe this curve geometrically (Fig. 9).

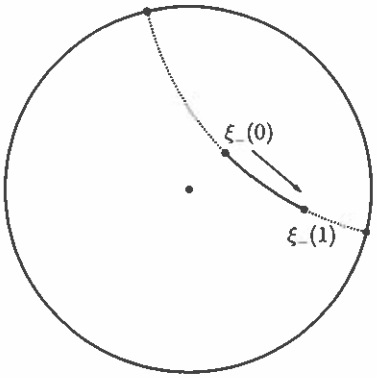

Figure 9: For linear interpolation, the fixed point ξ_- traces a hyperbolic line.

We restrict our attention to a particular example. We fix ω and pick $\alpha(t) = (1-t)\alpha_0 + t\alpha_1$, a linear interpolation between an initial value α_0 and a final value α_1.

Theorem 7. *For the linear interpolation described above, $\xi_-(t)$ traces a hyperbolic line segment.*

Proof. Recalling that $\xi_\pm(t)$ are circular inverses of each other, it suffices to show that $\xi_\pm(t)$ lies on a circle, and orthogonality with the unit circle follows. A rotation $\alpha \mapsto e^{is}\alpha$ rotates the corresponding fixed points as $\xi_\pm(t) \mapsto e^{-is}\xi_\pm(t)$. Since rotations preserve circles, we can without loss of generality assume that $\alpha(t)$ is a line parallel with the real axis, i.e. has the form

$$\alpha(t) = (1-t)a_0 + ta_1 + ib.$$

Computing $|\xi_\pm(t) + i\omega/b|^2$, we get

$$\left| \frac{\omega \pm \sqrt{\omega^2 - |\alpha(t)|^2}}{\alpha(t)} + \frac{i\omega}{b} \right|^2 = \frac{\omega^2}{b^2} - 1.$$

The right hand side is positive by the assumption that $\omega^2 > |\alpha|^2$, so $\xi_\pm(t)$ indeed lies on a circle with center $-i\omega/b$ and radius $\sqrt{(\omega^2/b^2) - 1}$. □

A Geometry of squeezed states

We will use an alternative formula for the hyperbolic distance,

$$d_h(z,w) = \operatorname{arcosh}(1 + 2\delta(z,w)), \quad \delta(z,w) = \frac{|z-w|^2}{(1-|z|^2)(1-|w|^2)}. \tag{74}$$

We recall the Poincaré metric, the metric induced by d_h,

$$g_h = 4\frac{1}{(1-|z|^2)^2}|\mathrm{d}z|^2.$$

The projective space of $\mathcal{H}$ has a natural Fubini-Study metric induced by the Hilbert-Schmidt distance

$$\|P-Q\|^2 = 4\,\mathrm{tr}((P-Q)^2)$$

between rank one projections P and Q. The factor of 4 is a convenient normalization. The sub-manifold of squeezed states $\mathcal{C}$ inherits the Fubini-Study metric

$$g_{FS} = 4\,\mathrm{tr}(dP(z)dP(z)),$$

where $P(z) = |\psi(z)\rangle\langle\psi(z)|$ are projections on $[\psi(z)]$. Again, the factor of 4 is non-standard normalization that fits our problem.

These two manifolds are congruent.

Theorem 8. *The map F is an isometric immersion of (D, g_h) into $(\mathcal{C}, g_{FS})$. In particular, the manifold of squeezed states is a model of hyperbolic geometry.*

This theorem is not new, see e.g. [3]. For completeness we include the proof. We follow [3] with only small changes.

We compute the Hilbert-Schmidt distance of squeezed states.

Lemma 9. *For any $z, w \in D$, we have*

$$\mathrm{tr}\left((P(z)-P(w))^2\right) = 2(1-(1+\delta(z,w))^{-\frac{1}{2}}).$$

Proof. In the proof we will use the standard Fock basis $|n\rangle$ obtained from $|0\rangle := \psi(0)$, and by the recursive relation $a^*|n\rangle = \sqrt{n+1}|n+1\rangle$. We claim that

$$\psi(z) = (1-|z|^2)^{\frac{1}{4}}\tilde{\psi}(z), \quad \tilde{\psi}(z) = e^{-\frac{1}{2}za^{*2}}\psi(0). \tag{75}$$

Indeed, using

$$e^{-\frac{1}{2}za^{*2}}ae^{\frac{1}{2}za^{*2}} = a + za^*,$$

we check that

$$(a+za^*)\tilde{\psi}(z) = 0.$$

To compute the normalization, we expand $\tilde{\psi}(z)$ in a Taylor series,

$$\tilde{\psi}(z) = \sum_{n=0}^{\infty}\left(-\frac{1}{2}\right)^n\frac{z^n}{n!}\sqrt{(2n)!}|2n\rangle.$$

Then

$$\langle\tilde{\psi}(z)|\tilde{\psi}(w)\rangle = \sum_{n=0}^{\infty}\frac{1}{4^n}\frac{(\bar{z}w)^n}{n!^2}(2n)! = (1-\bar{z}w)^{-\frac{1}{2}},$$

and using this for $z = w$ shows (75). To compute the Hilbert-Schmidt distance we use

$$\mathrm{tr}\left((P(z) - P(w))^2\right) = 2 - 2\,\mathrm{tr}(P(z)P(w)),$$

and

$$\mathrm{tr}(P(z)P(w)) = |\langle\psi(z)|\psi(w)\rangle|^2 = (1-|z|^2)^{\frac{1}{2}}(1-|w|^2)^{\frac{1}{2}}|1-\bar{z}w|^{-1}.$$

The expression in the lemma then follows from the identity

$$|1-\bar{z}w|^2 = |z-w|^2 + (1-|z|^2)(1-|w|^2),$$

and the definition of $\delta(z,w)$. □

Taylor expansion implies that

$$\mathrm{tr}\left((P(z) - P(w))^2\right) = \delta(z,w) + o(\delta(z,w)).$$

Comparing this with the hyperbolic distance, we get

$$\mathrm{tr}\left(((P(z) - P(w))^2\right) = \frac{1}{4}d_h(z,w)^2 + o(\delta(z,w)).$$

This implies that $g_h = g_{FS}$ as claimed in the theorem.

Acknowledgements

I would like to thank Dr. Martin Fraas and Tina Tan for their contributions to the original paper with the same name. Without them, this thesis would not exist. The original parts of this thesis include all of section 2, excluding subsection 2.4, and including everything after eq. 58. I would also like to thank the geometry group in QMAP for listening to my talk on my paper, which helped me tremendously in understanding Arthur Jiang, Chen Liang, and Tiching Kao for helping me proofread this paper.

References

[1] J. Avron and O. Kenneth. Entanglement and the geometry of two qubits. *Annals of Physics*, 324(2):470–496, 2009.

[2] J. Avron and O. Kenneth. An elementary introduction to the geometry of quantum states with pictures. *Reviews in Mathematical Physics*, 32(02):2030001, 2020.

[3] S. Bachmann, M. Fraas, and G. M. Graf. Dynamical crossing of an infinitely degenerate critical point. *Annales Henri Poincaré*, 18:1755–1776, 2017.

[4] I. Bengtsson and K. Życzkowski. *Geometry of quantum states: an introduction to quantum entanglement.* Cambridge university press, 2017.

[5] F. Bloch. Nuclear induction. *Physical review*, 70(7-8):460, 1946.

[6] M. Born and V. Fock. Beweis des Adiabatensatzes. *Zeitschrift für Physik*, 51(3-4):165–180, 1928.

[7] R. P. Feynman, F. L. Vernon Jr, and R. W. Hellwarth. Geometrical representation of the schrödinger equation for solving maser problems. *Journal of applied physics*, 28(1):49–52, 1957.

[8] R. J. Glauber. Coherent and incoherent states of the radiation field. *Physical Review*, 131(6):2766, 1963.

[9] D. Hilbert. *Über Flächen von konstanter Gaußscher Krümmung*, pages 437–448. Springer Berlin Heidelberg, Berlin, Heidelberg, 1970.

[10] T. Kato. On the adiabatic theorem of quantum mechanics. *J. Phys. Soc. Japan*, 5:435–439, 1950.

[11] A. Marden. *Hyperbolic Manifolds: An Introduction in 2 and 3 Dimensions*, chapter 1. Cambridge University Press, 2016.

[12] T. Needham. *Visual Complex Analysis.* Clarendon Press, 1997.

[13] U. Shackerley-Bennett, A. Pitchford, M. G. Genoni, A. Serafini, and D. K. Burgarth. The reachable set of single-mode quadratic hamiltonians. *Journal of Physics A: Mathematical and Theoretical*, 50(15):155203, 2017.